ANALYTICAL SCIENCES APRIL 2016, VOL. 32

Magnetic Nanoparticles-based Aptasensor Using Gold Nanoparticles as Colorimetric Probes for the Detection of *Salmonella typhimurium*

Nuo DUAN,*† Baocai XU, Shijia WU,* and Zhouping WANG**†**

**State Key Laboratory of Food Science and Technology, Synergetic Innovation Center of Food Safety and Nutrition, School of Food Science and Technology, Jiangnan University, Wuxi 214122, China*
***State Key Laboratory of Meat Processing & Quality Control, Yurun Group, Nanjing 210041, China*

This paper presents a sensitive and convenient visual methodology for *Salmonella typhimurium* detection using gold nanoparticles (AuNPs) as colorimetric probes and magnetic nanoparticles (MNPs) as concentration elements. In the protocol, the aptamers were first immobilized onto the surface of AuNPs and MNPs, respectively. Then, *S. typhimurium* were added into the above solution and incubated for 45 min. During the incubation, aptamer on the surface of nanoparticles could specifically bind to the target and form a MNPs-aptamer-*S. typhimurium*-aptamer-AuNPs sandwich structure complex. In a magnetic field, the formed complexes were easily separated from the solution, resulting in a fading of the AuNPs suspension and a decrease of the ultraviolet visible (UV/Vis) signal. The assay shows a linear response toward *S. typhimurium* concentration through a range of 25 to 10^5 cfu/mL, and the detection limit was improved to 10 cfu/mL. The applicability of the bioassay in real food samples was also investigated; the results were consistent with the experimental results obtained from plate-counting methods. It is believed that the developed aptasensor will broaden the application in bioassays.

Keywords *S. typhimurium*, aptamer, gold nanoparticles, magnetic nanoparticles, colorimetric assay

(Received October 7, 2015; Accepted December 7, 2015; Published April 10, 2016)

Introduction

Salmonella is one of the most frequent causes of foodborne outbreaks of gastroenteritis.[1,2] Among nearly 2500 serotypes of *Salmonella* reported, *Salmonella typhimurium* is the number one leading serotype causing salmonellosis worldwide.[3] The transmission of *S. typhimurium* is primarily through the consumption of raw or uncooked vegetables, poultry, and eggs.[4] The most common symptoms are characterized by: headache, vomiting, diarrhea and fever. On a global scale, *Salmonella* causes around 93.8 million gastroenteritis-related infections, resulting in 155000 deaths each year.[5] This increasing incidence of *S. typhimurium* in different food products attracts the government attention. The food safety regulations of some countries (*e.g.* China, USA) require no tolerance of *S. typhimurium* in ready-to-eat food. Therefore, sensitive detection methods for *S. typhimurium* are necessary for the proper regulation of food hygiene. The existing common detection methods include culture-based methods, molecular methods of regular and real-time polymerase chain reaction (PCR),[6,7] and immunoassay methods.[8–10] Despite many advances in these fields, it is still a challenge to find new approaches that could improve the simplicity, selectivity, stability and sensitivity of these analytical methods.

† To whom correspondence should be addressed.
E-mail: wangzp1974@163.com

Aptamer has received tremendous attention in analytical application as a recognition element due to their high affinity and specificity to a broad range of targets. Aptamer was obtained through *in vitro* selection or the systematic evolution of ligands by exponential enrichment (SELEX).[11,12] Compared with conventional antibodies, aptamers show many advantages, such as more chemically stable, inexpensive, simple to be chemically modified, and so on.[13] This made aptamer probes more flexible in design various types of biosensors, including fluorescence,[14,15] chemiluminescence,[16,17] electrochemical,[18,19] or colorimetric sensors.[20,21] Among these, colorimetry aptasensor, especially gold nanoparticles based colorimetry aptasensor, has attracted much attention owing to their conveniences of visual observation and simple operations. That is because gold nanoparticles possess unique properties, including good biocompatibility, excellent optical performance, special catalytic activity and the convenience of controlled fabrication.[22,23] Aptamers could absorb onto the AuNPs by electrostatic absorption or chemical bonding. When AuNPs aggregate, the color of AuNPs solutions changes from red to blue and the surface plasmon band broadens and shifts to a longer wavelength. Magnetic nanoparticles (MNPs) are also one of the most popular separation materials, which have been extensively implemented in the fields of DNA hybridization analysis, immunoassays, protein and enzyme immobilization, cell separation, and drug delivery.[24,25] Thus, it is very encouraging to combine AuNPs and MNPs for developing the *S. typhimurium* detection method.

In this paper, we herein report a novel colometric method for

rapid and sensitive detection of *S. typhimurium* using aptamer as a specific recognition element, AuNPs as an indicator, and MNPs as a concentration element. In this approach, AuNPs and MNPs labeled *S. typhimurium via* aptamer-target interaction formed a MNPs-aptamer-target-aptamer-AuNPs complex and accumulated in the MNPs. Then, this formed complex can be separated by an external magnetic field, resulting in fading in the color of AuNPs suspension. *S. typhimurium* were detected according to the decrease in the UV-Vis absorbance. This method was successfully applied to detect *S. typhimurium* in spiked milk samples.

Experimental

Reagents and chemicals

Chloroauric acid ($HAuCl_4$) and streptavidin were obtained from Sigma-Aldrich (USA). Trisodium citrate, 1,6-hexanediamine, anhydrous sodium acetate, $FeCl_3{\cdot}6H_2O$, glycol, and 25% glutaraldehyde ($OHC(CH_2)_3CHO$) were of analytical grade and were purchased from Sinopharm Chemical Reagent Co., Ltd. (Shanghai, China). The *S. typhimurium* aptamer were prepared in our laboratory.[26] The sequence of *S. typhimurium* aptamer is 5′-SH-ATAGGAGTCACGACGAC-CAGAAAGTAATGCCCGGTAGTTATTCAAAGATGAGTAG-GAAAAGATATGTGCGTCTACCTCTTGACTAAT-3′ (apt1), and 5′-Bio-ATAGGAGTCACGACGACCAGAAAGTAATGCC-CGGTAGTTATTCAAAGATGAGTAGGAAAAGATATGTGC-GTCTACCTCTTGACTAAT-3′ (apt2), synthesized by the Shanghai Sangon Biological Science & Technology Company (Shanghai, China).

Apparatus

UV-Vis absorption spectra were recorded using a UV-1800 spectrophotometer (Shimadzu Co., Japan). Transmission electron microscopy (TEM) measurement was made on a JEOL Model 2100HR instrument operating at 200 kV accelerating voltage (TEM, JEOL Ltd., Japan). The FT-IR spectra of the nanoparticles were measured using a Nicolet Nexus 470 Fourier-transform infrared spectrophotometer (Thermo Electron Co., USA). Ultrapure water of resistivity 18.2 MΩ/cm was obtained from a Milli-Q Water System (Millipore Corp., Bedford, MA, USA) and was used throughout for the preparation of solutions.

Bacterial strains and culture media

The *S. typhimurium* ATCC 14028 was kindly provided by the Animal, Plant and Food Inspection Centre, Jiangsu Entry-Exit Inspection and Quarantine Bureau (Nanjing, China). Bacteria were grown in LB media overnight past the logarithmic phase. Cells were pelletized at 3000 rpm and 4°C and washed twice in a 1 × binding buffer (50 mM Tris–HCl at pH 7.4, 5 mM KCl, 100 mM NaCl, and 1 mM $MgCl_2$) at room temperature. After incubation at 37°C for 18 h, the number of viable cells was determined by a microbial plate count method.

Synthesis of AuNPs

The AuNPs were prepared using a trisodium citrate reduction method. Prior to the synthesis, all glassware used in the following procedures was cleaned in a bath of freshly prepared HNO_3/HCl (3:1, v/v), rinsed thoroughly in ultrapure water, and dried prior to use. Briefly, $HAuCl_4$ solution (4.2 mL, 1%) and ultrapure H_2O (95.8 mL) were heated to boiling point for 10 min with vigorously stirring. Then, trisodium citrate (10 mL, 1%) was rapidly added, and the solution was boiled continually for 15 min, during which time a color change from blue to red-violet was observed. The heating source was removed, and the colloid was kept at room temperature for another 15 min and then stored at 4°C.

Synthesis of MNPs

The amine-functionalized MNPs were prepared *via* a modified method, as described in a previous report.[27] Briefly, 1,6-hexanediamine (6.5 g), anhydrous sodium acetate (2.0 g) and $FeCl_3{\cdot}6H_2O$ (1.0 g) were first dissolved in glycol (30 mL) under stirring vigorously at 50°C to give a transparent solution. This solution was then transferred into a Teflon-lined autoclave and reacted at 198°C for 6 h. With the completion of the reaction, an external magnet was used to separate the nanoparticles from the sample solution. The black products were then washed repeatedly with water and ethanol to remove untreated impurities and then dried at 50°C before characterization and application.

AuNPs-apt1 and MNPs-apt2 conjugates preparation

Aptamer functionalized AuNPs were prepared *via* the well-known gold-sulfur chemistry. The AuNPs-apt1 conjugates were synthesized according to the literature with minor modification.[28] That is, 5 μL of apt1 (100 μM) were added into 1 mL of the AuNPs solution. After 16 h of incubation at room temperature, the AuNPs-apt1 complex was aged with salts (0.1 M NaCl, 0.1 mM phosphate, pH 7.0) for 40 h to complete the self-assembly of aptamer onto the surface of AuNPs. Then, the conjugates were centrifuged at 12500 rpm at room temperature for 15 min twice to remove the free aptamer. The final deposition was resuspended in 1 mL of 1 × binding buffer for further use.

The immobilization of aptamer onto MNPs was carried out on, briefly, 5 mg of the MNPs was dispersed in 5 mL of 10 mM phosphate buffer solution (PBS, pH 7.4), followed by the addition of 1.25 mL of 25% glutaraldehyde and reacted for 2 h at room temperature with slowly shaking. After magnetic separation, the MNPs were dispersed in 5 mL of 10 mM PBS, and 100 μL of 1.0 mg/mL streptavidin was added. The mixture was shaken slowly at room temperature for 12 h. The streptavidin coated MNPs were separated and washed with PBS for three times. Then, 5 μL of 100 μM apt2 was introduced into the collected MNPs (1 mg/mL). The resulting mixture was incubated for 2 h at 37°C under gentle mixing. The mixture was washed with PBS twice and magnetically separated. The supernatant was removed and MNPs-apt2 conjugates resuspended in 1 mL of 1 × binding buffer for further use.

Colorimetric detection of S. typhimurium

During the colorimetric detection of *S. typhimurium*, different concentrations of *S. typhimurium* were added to AuNPs-apt1 conjugates (300 μL) and MNPs-apt2 conjugates (80 μL) and incubated for 45 min at room temperature. The samples were ready for detection after 10 s of adsorption with an external magnet. A color change was observed with the naked eyes, and the absorbance spectra were assayed using the UV-1800 spectrophotometer.

Sample preparation

A 5-mL portion of a milk sample was centrifuged at 7000 rpm for 10 min at 10°C, and the upper layer of cream was removed. The supernatant was subsequently filtered through a 0.45-μm filtration membrane after diluted with ultrapure water at a 1:20 ration. Different *S. typhimurium* concentrations were then added to the prepared samples for the experiments.

Results and Discussion

Principle of S. typhimurium detection

The schematic illustration of the methodology for *S. typhimurium* determination with aptamer as a recognition element, colorimetric AuNPs as an indicator, and MNPs as concentration elements is shown in Fig. 1. Biotin modified aptamer responding to *S. typhimurium* were first assembled onto the surface of streptavidin activated MNPs *via* streptavidin-biotin specific binding. A thiol modified *S. typhimurium* aptamer was immobilized on the surface of AuNPs through a Au–S bond interaction. In the absence of a target, the AuNPs-apt1 and MNPs-apt2 were dispersed in solution, and appeared wind red. In the presence of a target, due to the high affinity of aptamer to the corresponding target, *S. typhimurium* were labeled by AuNPs-apt1 and MNPs-apt2, and formed a sandwich structure of AuNPs-apt1-target-MNPs-apt2. Then this formed complex can be separated by the external magnetic field, resulting in fading in the color of AuNPs suspension and a decrease in the UV-Vis absorbance. The method based on this concept should be very sensitive because MNPs have excellent separation and concentration ability and AuNPs have a high extinction coefficient.

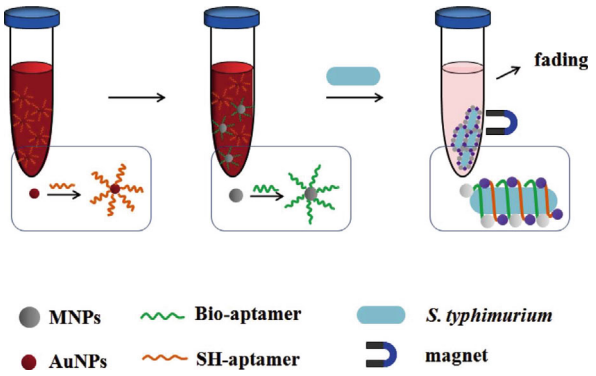

Fig. 1 Schematic illustration of the strategy for *S. typhimurium* detection using aptamer modified AuNPs and MNPs.

Characterization of AuNPs and MNPs

The morphology of AuNPs was determined by TEM, which showed that the obtained particles were spherical and well proportioned with an average diameter at about 13 nm (Fig. 2A). As shown in Fig. 2B, the AuNPs displayed a strong absorption band at approximately 520 nm. The TEM image of MNPs (Fig. 2C) demonstrated a good dispersibility and morphology of MNPs. The FT-IR spectroscopy of MNPs is depicted in Fig. 2D. The characteristic bands at 1635, 1400, 1052/cm were assigned to the amino group. The strong IR band at 583/cm is attributed to the Fe–O vibrations. The result indicated that the MNPs had been functionalized with amino groups in the synthetic process.

Characterization of the AuNPs-apt1 and MNPs-apt2 conjugates

To comfirm that the aptamers were successfully immobilized onto the surface of AuNPs and MNPs, respectively, UV-vis absorption spectroscopy was used to monitor the reaction products; the results are shown in Fig. 3. The strong absorbance of aptamers before conjugation to nanoparticles can be seen at 260 nm (Fig. 3, curve a and b). After the incubation of AuNPs and apt1, and MNPs and apt2, the supernatant was collected by centrifugation and magnetic separation. The result showed that the absorbance of the supernatant liquor is weaker at 260 nm

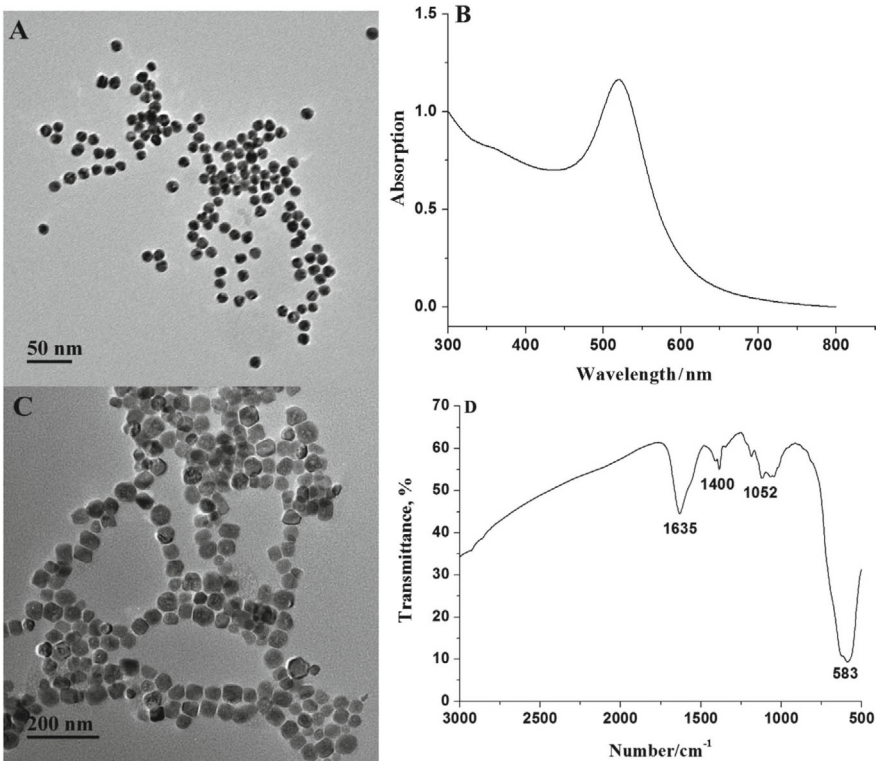

Fig. 2 TEM image (A) and UV-vis absorption spectra (B) of AuNPs, TEM image (C) and FT-IR spectrum (D) of MNPs.

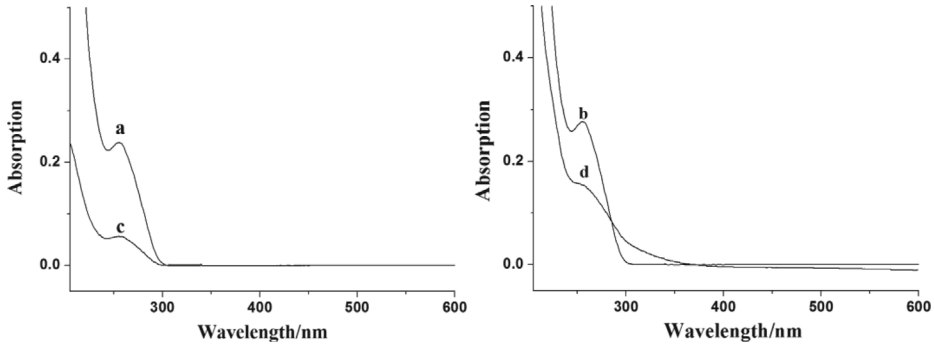

Fig. 3 UV-vis absorption spectra of the initial aptamer solution (a, b), supernatant liquor after aptamer conjugation to AuNPs (c) and MNPs (d).

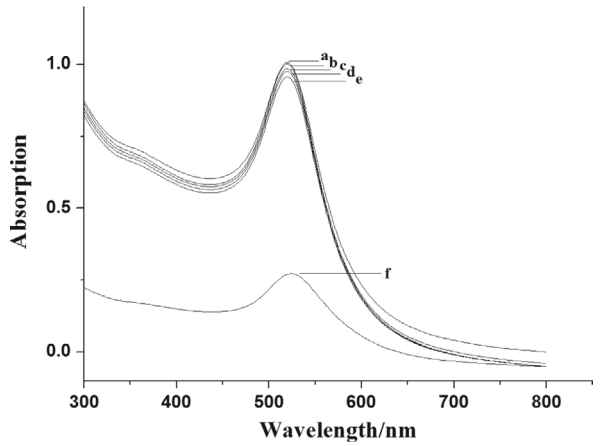

Fig. 4 UV-vis absorption spectra of AuNPs (a), AuNPs-apt1 (b), AuNPs + MNPs (c), AuNPs-apt1 + MNPs-apt2 (d), AuNPs + MNPs + *S. typhimurium* (e), AuNPs-apt1 + MNPs-apt2 + *S. typhimurium* (f). The concentration of *S. typhimurium* was 10^4 cfu/mL.

(Fig. 3, curve c and d), which verified that the aptamers has been successfully conjugated to the AuNPs and MNPs.

Control experiment

To confirm that the fading of AuNPs was caused by the sandwich structure of AuNPs-apt1-target-MNPs-apt2, several control experiments were carried out. As shown in Fig. 4 curve a, the AuNPs solution exhibit an absorption peak at 520 nm. The absorbance of AuNPs did not change significantly after aptamer labeling, meaning that this modification does not affect the properties of the AuNPs (curve b). The no obvious difference among the curve c, d and e indicated that AuNPs or AuNPs-apt1 did not absorb onto the surface of MNPs or MNPs-apt2, and the target did not bind to AuNPs or MNPs. However, the strong absorbance of AuNPs at 520 nm decreased significantly, and the red color disappeared upon the addition of target bacteria (Fig. 4 curve f). The results indicate that the binding of aptamers and target is related to the highly efficient fading of AuNPs.

Optimization for the assay

According to the experimental scheme, both the AuNPs-apt1 and MNPs-apt2 conjugates contribute to the UV-Vis absorption. When the AuNPs-apt1 conjugates concentration is too high, it is unsuitable for detection of small amounts of the target because too large a background is present. While, if the MNPs-apt2 conjugates concentration is too low, a larger amount AuNPs-apt1 conjugates would dissociate in the solution, also resulting in an enhanced background. Thus, it is necessary to investigate the concentration of these conjugates. The results showed that the assay response was optimal with 300 μL AuNPs-apt1 conjugates and 80 μL MNPs-apt2 conjugates (Fig. 5).

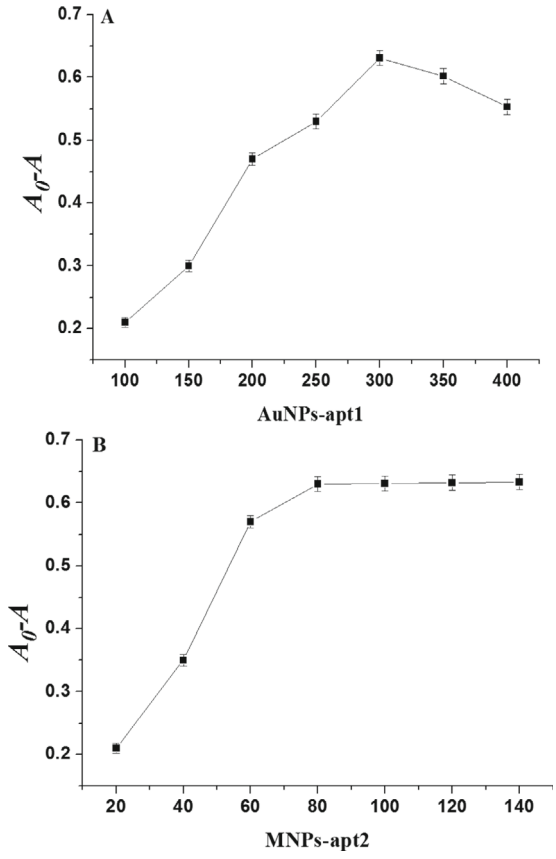

Fig. 5 Effect of the concentration of AuNPs-apt1 (A) and MNPs-apt2 conjugates (B) on the relative absorbance (A_0–A) of the assay. The concentration of *S. typhimurium* was 10^4 cfu/mL.

Quantitative analysis of the developed method

To demonstrate the performance of the aptasensor for the visual detection of *S. typhimurium* by the principle mentioned above, different concentrations of *S. typhimurium* were

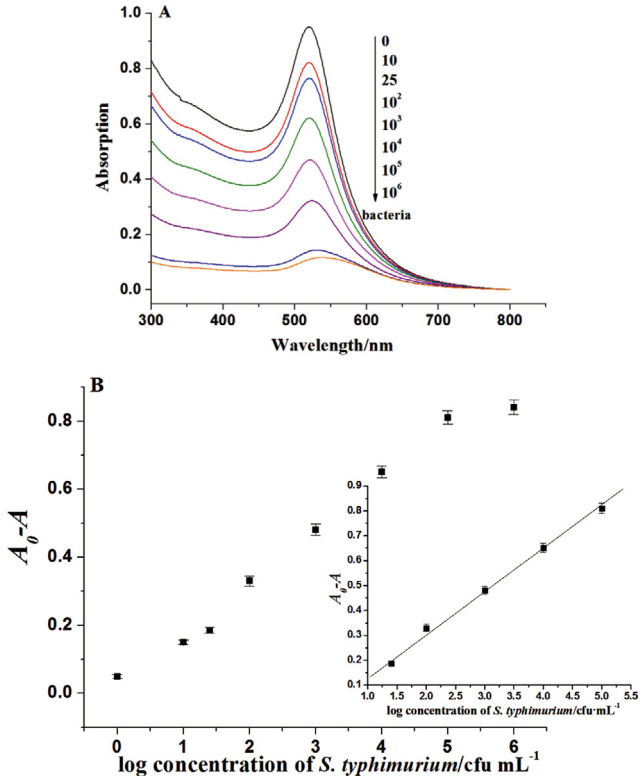

Fig. 6 Absorbance response for different concentrations of *S. typhimurium* (A), and a corresponding plot of the relative absorbance (A_0–A) *versus S. typhimurium* concentration (B) measured by the developed method.

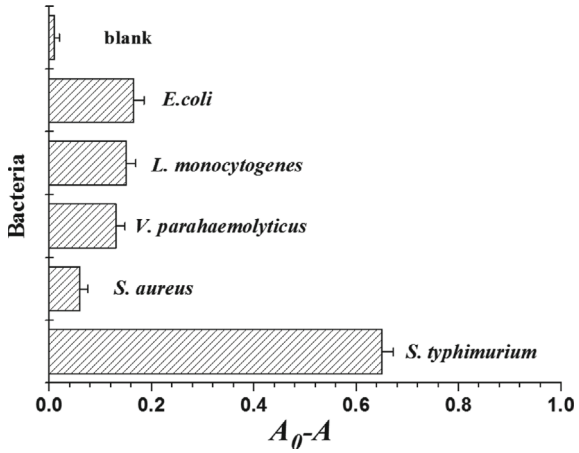

Fig. 7 Specificity evaluation of the developed method for *S. typhimurium* (10^4 cfu/mL), and against other bacteria (10^5 cfu/mL) and blank, respectively.

Table 1 Quantification of *S. typhimurium* cells in the spiked milk samples by the developed method

Sample	Spiked concentration by counting method/ cfu mL^{-1}	Measured concentration by developed method/ cfu mL^{-1} (mean ± SD)
Milk 1	2.0×10^2	$(1.9 \pm 0.11) \times 10^2$
Milk 2	2.0×10^3	$(2.0 \pm 0.13) \times 10^3$
Milk 3	2.0×10^4	$(2.0 \pm 0.08) \times 10^4$
Milk 4	2.0×10^5	$(1.9 \pm 0.12) \times 10^5$

SD: Standard deviation (n = 5).

analyzed. Figure 6A shows the representative UV-Vis signal of different concentrations of *S. typhimurium* by the developed method. The result clearly demonstrated that the higher was the concentration of *S. typhimurium* added, the more was *S. typhimurium* captured; the absorption peak at 520 nm of AuNPs decreased gradually. Under the optimal conditions, the logarithm of the *S. typhimurium* concentration is proportional to the decreased absorbance (ΔA) in which ΔA represents the AuNPs absorbance in the absence (A_0) and in the presence of *S. typhimurium* (A) in the range of 25 – 10^5 cfu/mL; the detection limit was improved to 10 cfu/mL. The regression equation was $y = 0.1699x - 0.0314$ ($R = 0.9980$), where y was the UV-Vis absorbance, and x was the logarithm concentration of *S. typhimurium*. Compared to many different detection methods for *S. typhimurium* (see Supporting Information Table S1), our method displayed excellent sensitivity and linearity for quantitative detection.

Specificity and analytical application of the assay

The assay specificity for *S. typhimurium* was evaluated by selecting other bacteria as the interfering bacteria, such as *Staphylococcus aureus*, *Vibrio parahaemolyticus*, *Listeria monocytogenes*, and *Escherichia coli*. Figure 7 shows the response of the absorbance change at 520 nm after incubation with these bacteria. As is vividly indicated in Fig. 7, *S. typhimurium* reveals a much stronger response of ΔA_{520} than the other bacteria. It is suggested that this colorimetric aptasensor response to its target *S. typhimurium* has good specificity. In order to demonstrate the practical applicability of the developed method for determination of *S. typhimurium* in real samples, artificially *S. typhimurium* contaminated milk samples spiked with different concentration levels were detected. The results are summarized in Table 1 and show good agreement with both the expected and found values.

Conclusion

In summary, a simple and sensitive optical system for *S. typhimurium* detection based on AuNPs and MNPs has been developed, which employs aptamer as a recognition element. This aptamer-based assay demonstrated several advantages. The stable and high affinity and specificity ability of aptamers contribute to the high selectivity. Gold nanoparticles exhibit excellent optical characteristics to assure the high sensitivity. Magnetic nanoparticles for separation brought about the convenience and low detection limit of the target. The assay also provides a promise for the easy and sensitive detection of other targets after substituting the corresponding aptamer. Due to this simple, specificity and cost-effective of this protocol, we believe that this assay can be expected to open up new opportunities for biological applications.

Acknowledgements

This work was partially supported by the National Science and Technology Support Program of China (2015BAD17B02-5), NSFC 31401575, NSFC 31401576, and JUSRP51309A.

References

1. J. Farkas, *Int. J. Food Microbiol.*, **1998**, *44*, 189.
2. K. C. Sarjeant, S. K. Williams, and A. Hinton, *Poultry Sci.*, **2005**, *84*, 955.
3. E. Galanis, D. M. A. Lo Fo Wong, M. E. Patrick, N. Binsztein, A. Cieslik, T. Chalermchikit, A. Aidara-Kane, A. Ellis, F. J. Angulo, and H. C. Wegener, *Emerg. Infect. Dis.*, **2006**, *12*, 381.
4. N. F. Crum-Cianflone, *Curr. Gastroenterol. Rep.*, **2008**, *10*, 424.
5. S. E. Majowicz, J. Musto, E. Scallan, F. J. Angulo, M. Kirk, S. J. O'Brien, T. F. Jones, A. Fazil, and R. M. Hoekstra, *Clin. Infect. Dis.*, **2010**, *50*, 882.
6. M. K. Park, K. A. Weerakoon, J. H. Oh, and B. A. Chin, *Food Control*, **2013**, *33*, 330.
7. D. M. Prendergast, D. Hand, E. N. Ghallchoir, E. McCabe, S. Fanning, M. Griffin, J. Egan, and M. Gutierrez, *Int. J. Food Microbiol.*, **2013**, *166*, 48.
8. I. H. Cho and J. Irudayaraj, *Int. J. Food Microbiol.*, **2013**, *164*, 70.
9. J. Bang, S. Shukla, Y. H. Kim, and M. Kim, *Rom. Biotech. Lett.*, **2012**, *17*, 7194.
10. A. G. Mantzila, V. Maipa, and M. I. Prodromidis, *Anal. Chem.*, **2008**, *80*, 1169.
11. C. Tuerk and L. Gold, *Science*, **1990**, *249*, 505.
12. A. D. Ellington and J. W. Szostak, *Nature*, **1990**, *346*, 818.
13. S. M. Nimjee, C. P. Rusconi, B. and A. Sullenger, *Annu. Rev. Med.*, **2005**, *56*, 555.
14. Q. Zhao, Q. Lv, and H. L. Wang, *Anal. Chem.*, **2014**, *86*, 1238.
15. Y. Jin, J. Y. Bai, and H. Y. Li, *Analyst*, **2010**, *135*, 1731.
16. L. Park, J. L. Kim, and J. H. Lee, *Talanta*, **2013**, *116*, 736.
17. W. B. Shim, H. Mun, H. A. Joung, J. A. Ofori, D. H. Chung, and M. G. Kim, *Food Control*, **2014**, *36*, 30.
18. M. Hua, M. L. Tao, P. Wang, Y. F. Zhang, Z. S. Wu, Y. B. Chang, and Y. H. Yang, *Anal. Sci.*, **2010**, *26*, 1265.
19. L. R. Schoukroun, S. Wagan, and R. J. White, *Anal. Chem.*, **2014**, *86*, 1131.
20. Z. B. Chen, Y. Q. Huang, X. X. Li, T. Zhou, H. Ma, H. Qiang, and Y. F. Liu, *Anal. Chim. Acta.*, **2013**, *787*, 189.
21. K. M. Song, E. Jeong, W. Jeon, M. Cho, and C. Ban, *Anal. Bioanal. Chem.*, **2012**, *402*, 2153.
22. W. A. Zhao, W. Chiuman, J. C. F. Lam, S. A. McManus, W. Chen, Y. G. Cui, R. Pelton, M. A. Brook, and Y. F. Li, *J. Am. Chem. Soc.*, **2008**, *130*, 3610.
23. D. Kumar, N. Saini, N. Jain, R. Sareen, and V. Pandit, *Expert Opin. Drug Del.*, **2013**, *10*, 397.
24. C. R. Tamanaha, S. P. Mulvaney, J. C. Rife, and L. Whitman, *Biosens. Bioelectron.*, **2008**, *24*, 1.
25. S. J. Son, J. Reichel, B. He, M. Schuchman, and S. B. Lee, *J. Am. Chem. Soc.*, **2005**, *127*, 7316.
26. N. Duan, S. J. Wu, X. J. Chen, Y. K. Huang, Y. Xia, X. Y. Ma, and Z. P. Wang, *J. Agric. Food Chem.*, **2013**, *61*, 3229.
27. L. Y. Wang, L. Wang, F. Zhang, and Y. D. Li, *Chem.—Eur. J.*, **2006**, *12*, 6341.
28. R. Elghanian, J. J. Storhoff, R. C. Mucic, R. L. Letsinger, and C. A. Mirkin, *Science*, **1997**, *277*, 1078.